NACA RM E53D09

NACA

RESEARCH MEMORANDUM

INTERNAL PERFORMANCE CHARACTERISTICS OF VARIABLE-THROAT PLUG- AND VANED-TYPE CONVERGENT-DIVERGENT NOZZLES

By H. George Krull, Fred W. Steffen, and Carl C. Ciepluch

Lewis Flight Propulsion Laboratory
Cleveland, Ohio

NATIONAL ADVISORY COMMITTEE
FOR AERONAUTICS

WASHINGTON

June 23, 1953
Declassified April 15, 1958

NATIONAL ADVISORY COMMITTEE FOR AERONAUTICS

RESEARCH MEMORANDUM

INTERNAL PERFORMANCE CHARACTERISTICS OF VARIABLE-THROAT PLUG- AND VANED-TYPE CONVERGENT-DIVERGENT NOZZLES

By H. George Krull, Fred W. Steffen, and Carl C. Ciepluch

SUMMARY

As part of an over-all program for the experimental investigation of large-scale jet nozzles, the internal performance characteristics of three types of variable-throat convergent-divergent nozzles were obtained over a wide range of pressure ratios. The experimental results obtained with one of these nozzles was applied to a typical flight plan of a ram-jet missile.

There were only small differences in peak thrust coefficient between the three types of variable-throat convergent-divergent nozzles. The peak thrust coefficients obtained with these nozzles approached or equalled those obtained with several fixed-geometry convergent-divergent nozzles from a previous investigation. There was little gain (1 percent or less) obtained in the peak thrust coefficient of a convergent-divergent plug-type nozzle when the sharp corner of a simple conical center plug was rounded.

By proper matching of a variable-throat convergent-divergent nozzle to a typical flight plan of a ram-jet missile, a thrust coefficient of 0.95 was obtained over a flight Mach number range from 2.13 to 3.0. With the performance characteristics of the variable-throat nozzles investigated, this maximum thrust coefficient was obtained by matching the nozzle expansion ratio to the flight plan at the minimum flight Mach number and allowing the nozzle to operate underexpanded at the higher flight Mach numbers.

INTRODUCTION

It is important that the jet nozzle of a ram-jet or turbojet installation operating at supersonic speeds have high internal efficiency, because a small loss in nozzle efficiency results in a large loss in engine performance. The reason high efficiency is particularly

important at supersonic speeds (or high nozzle-pressure ratios) is that a small loss in jet thrust results in a large loss in net thrust.

In order that large changes in engine operating conditions (such as the fuel-air-ratio variation in a ram-jet or turbojet afterburner) can be provided for, a nozzle should have a variable throat. Maximum-internal-efficiency operation at high nozzle-pressure ratios (greater than 4) requires a convergent-divergent nozzle. Previous investigations of fixed-geometry convergent-divergent nozzles, reported in references 1 to 3, show that high peak thrust coefficients can be obtained at the design pressure ratios. Also, at the off-design condition, there are severe losses due to overexpansion or underexpansion of the nozzles.

As a first approach to the problem of providing a variable-geometry nozzle, three variable-throat convergent-divergent nozzles with fixed exits were investigated and are reported herein. It was recognized that this type of nozzle is not suitable to all flight plans because the expansion ratio cannot be varied independently of the throat area, but there are some applications such as ram-jets. To date no known experimental data are generally available for predicting the performance of large scale variable-throat convergent-divergent nozzles except in reference 4, which is a brief preliminary publication on one of the configurations presented herein.

The three variable-throat nozzles were of two basic types. Two of the nozzles were of simple conical construction with a conical center plug. Each had a throat-area variation from approximately 50 to 83 square inches with an attendant expansion-ratio variation from 1.5 to 2.5. The third nozzle was two dimensional with a series of fixed and movable vanes which formed convergent-divergent flow channels. The throat area of this nozzle could be varied from 52 to 84 square inches which resulted in an expansion-ratio variation from 1.45 to 2.34. Each nozzle was operated over a range of pressure ratios from 1.5 to at least the design pressure ratio for each of six expansion-ratio settings. The design pressure ratio is defined as the ideal nozzle pressure ratio required to completely expand the flow for a given physical expansion ratio.

APPARATUS AND INSTRUMENTATION

Installation

The nozzles were installed in a test chamber connected to the laboratory combustion air and altitude-exhaust facilities as shown in figures 1; 2(a), for the first part of the investigation; and 2(b), for the latter part. The nozzles were installed on a mounting pipe

freely supported on flexure plates in both installations; the pipe was connected through linkage to a calibrated balanced-air-pressure diaphragm for measuring thrust. A labyrinth seal around the upstream end of the mounting pipe, figure 2(a), and around the cylindrical section upstream of the diffuser inlet, figure 2(b), separated the nozzle inlet air from the exhaust and provided a means of maintaining a pressure difference across the nozzle.

During the first phase of the investigation, an examination of the data showed that the force measured on the balanced-air-pressure diaphragm with the test configuration shown in figure 2(a) was several times as large as the jet thrust of the nozzle. This condition was due to the large area of the mounting pipe at the labyrinth seal which resulted in a large pressure-area term in the thrust equation (see appendix). Ordinary experimental scatter was thus magnified several times. To correct this condition for the latter phase of the investigation, the inlet pipe was modified as shown in figure 2(b). The area under the new labyrinth seal was about 1/3 of the original area. With this modification, the measured force on the balanced-air-pressure diaphragm was of about the same magnitude as the nozzle jet thrust, and the scatter of the thrust data was considerably reduced.

The diffuser at the inlet to the mounting pipe had a cone half-angle of 20°. With this wide angle, the flow separated from the wall of the diffuser and caused the nozzle-inlet pressure to surge. A splitter cone was installed in the diffuser, which eliminated flow separation and pressure surge (fig. 2(b)).

Nozzles

The three variable-throat convergent-divergent nozzles which were investigated are shown in figures 3 and 4. The first nozzle, shown in figures 3(a) and 3(b), consisted of a movable convergent-divergent conical shell with a fixed conical center plug. This configuration will hereinafter be referred to as "the sharp-plug nozzle." The ratio of inlet to outlet area was about 1.0, and the throat area was varied by translating the movable shell axially downstream by means of the adjusting screws. Air leakage between the outer and the movable shells was prevented by means of a rubber tube pressurized with water as shown in figure 3(a). The throat area of the nozzle for any position of the movable shell was considered to be the annular area at the minimum diameter of the movable shell perpendicular to the axis of the nozzle. The second nozzle was the same as the first except that the sharp plug was replaced by the rounded plug shown in figure 3(c). Essentially, this plug differed from the sharp plug in that the sharp corner was rounded to a 2.46-inch radius. The maximum diameter was the same as that of the sharp plug. This nozzle will be referred to as the "rounded-plug nozzle." The third nozzle which also had an inlet to outlet area

ratio of 1 is shown in figures 4(a) and 4(b). This nozzle was two dimensional with a series of alternately fixed and movable vanes which formed convergent-divergent flow channels; it will be referred to as "the vaned nozzle." The throat area was varied by translating the movable vanes upstream by means of the adjusting screws. Each blade had a horizontal flat surface at the maximum thickness and the forward and rear surfaces of the blade were faired into this flat portion to a small radius. The throat was considered to be in a plane perpendicular to the axis of the nozzle at the leading edge of the flat surface of the fixed vanes as shown in figure 4(a).

It was characteristic of these nozzles that for any given throat area the nozzles had only one expansion ratio. The variation of throat area with expansion ratio, effected by translating the movable shell of the sharp-plug and rounded-plug nozzles or the movable vanes of the vaned nozzle over the entire range of travel, is shown in figure 5. Over the full range of throat areas, the expansion ratio varied from 1.5 to 2.5 for both the sharp-plug and rounded-plug nozzles and from 1.45 to 2.34 for the vaned nozzle. These nozzles were designed for an exit Mach number of about 2.4, and they were for exploratory purposes rather than for any specific flight plan.

Instrumentation

Pressures and temperatures were measured at the stations indicated in figures 2(a) and 2(b). The stations at which the instrumentation was installed in the test chamber with the original inlet pipe are shown in figure 2(a). At the mounting-pipe inlet, station 3, were 30 total-pressure and 14 static-pressure probes. A survey consisting of 14 total-pressure probes, 8 static-pressure probes, 2 wall static taps, and 6 thermocouples was located at the nozzle inlet, station 4, to measure air flow.

The stations at which the instrumentation was installed in the test chamber with the modified inlet pipe are shown in figure 2(b). At the diffuser inlet, station 2, a survey consisting of 8 total-pressure probes, 7 static-pressure probes, and 3 wall static taps was provided for measuring air flow. The nozzle inlet, station 4, was instrumented with 14 total-pressure probes and 6 thermocouples. A static-pressure survey was installed along the bellmouth and along the outside of the diffuser. Ambient-exhaust-pressure instrumentation was also provided at the exhaust-nozzle exit.

The sharp-plug nozzle was investigated in the test chamber shown in figure 2(a), and the rounded-plug and vaned nozzles were investigated with the test chamber modified as shown in figure 2(b). The sharp-plug and rounded-plug nozzles had 15 wall static taps located along the

length of the movable shell and 10 wall static taps along the plug. The vaned nozzle had 12 wall static taps located along one of the fixed vanes and 10 wall static taps along one of the movable vanes.

PROCEDURE

Nozzle-performance data were obtained over a range of pressure ratios at several different air flows. The pressure ratio across the nozzle was varied by holding the inlet pressure and temperature constant and lowering the exhaust pressure. Pressure ratio was varied from about 1.5 to at least the design pressure ratio for each of the six expansion-ratio settings of all three nozzles. With the size nozzles used for this investigation, it was necessary to heat the nozzle-inlet air to 910° R in order to cover the desired pressure ratio range with the laboratory facilities. Early in the investigation reported in reference 1, the distribution of nozzle-wall pressures was checked for evidence of condensation shock. No such evidence was found (see ref. 1).

The thrust coefficient was computed by dividing the actual jet thrust of the nozzle by the ideally obtainable jet thrust. The actual jet thrust was computed from measurements taken with the balanced-air-pressure diaphragm and pressure and temperature surveys throughout the test setup. The ideally obtainable jet thrust was the product of the measured mass flow and the jet velocity calculated by assuming isentropic expansion to the exhaust pressure. The symbols used in this report and the methods of calculation are given in the appendix.

RESULTS AND DISCUSSION

Performance Characteristics

Thrust coefficients. - It is shown in reference 1 that thrust coefficients ranging from 0.95 to 0.975 could be obtained with fixed-geometry convergent-divergent nozzles at design pressure ratios. These data were used as a basis of comparison for the three variable-throat convergent-divergent nozzles investigated. The thrust coefficients obtained with these nozzles are shown in figures 6(a) to 6(c) over a range of nozzle pressure ratios. As can be seen, these nozzles had peak thrust coefficients ranging from 0.945 to 0.975 over a range of pressure ratios from 6 to 16. These peak thrust coefficients approached or equalled those obtained with the fixed-geometry nozzles which are indicated by the solid symbols on the figures. The peak thrust coefficients did not always occur at the design pressure ratios; they also occurred at pressure ratios higher than design, and the reason for this will be discussed later in the text.

There were small variations in peak thrust coefficients between the three nozzles. The peak thrust coefficient of the sharp-plug nozzle varied from 0.945 to 0.965. The lowest peak thrust coefficient was obtained when the nozzle was set for an expansion ratio of 2.27. In this position, the flow area at the maximum diameter of the plug was only slightly larger than the throat of the nozzle; nearly critical flow therefore existed at the maximum diameter of the plug. With this high-velocity air flowing around the sharp corner of the plug, there was evidently a loss in total pressure with a resultant loss in thrust coefficient.

The peak thrust coefficients obtained with rounded-plug nozzle ranged from 0.949 to 0.975. For all expansion ratio settings except the maximum, this nozzle had peak thrust coefficients approximately equal to or 1 percent higher than the sharp-plug nozzle. For the maximum expansion-ratio setting, the sharp-plug nozzle had a peak thrust coefficient 1 percent higher than the rounded-plug nozzle which was in disagreement with the wall pressure surveys and is therefore presumed to be in error.

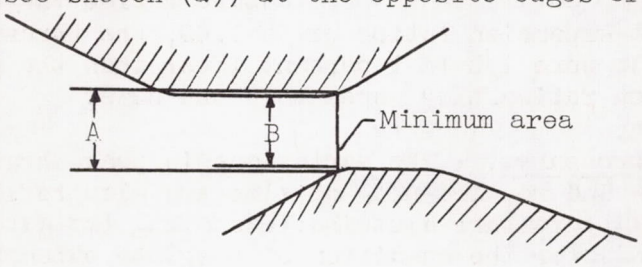
The vaned nozzle maintained an approximately constant peak thrust coefficient over the entire range of pressure ratios varying from 0.955 to 0.96. At expansion ratios up to 1.69, the thrust coefficients of the vaned nozzle were 1/2 to 1 percent lower than the plug nozzles. At higher expansion ratios, they were about the same.

Wall static pressures. - The variations in peak thrust coefficient between the sharp- and rounded-plug nozzles are also reflected in the measured wall-static-pressure distributions along the divergent walls of the movable shell for the condition of complete expansion as shown with the theoretical isentropic expansion in figures 7(a) to 7(f). The higher the integrated pressure along the divergent walls of a convergent-divergent nozzle for a given condition, the higher the thrust. Therefore, as was indicated by the thrust coefficients, except for the maximum expansion ratio, the pressures along the divergent walls of the movable shell were higher for the rounded-plug nozzle. Although not presented, the wall static pressures measured along the surfaces of the sharp and rounded plugs showed a corresponding effect. It can also be seen from figure 7 that, for each of the expansion-ratio settings, the wall-static-pressure ratio at the throat of the nozzle was lower than critical, ranging from 0.32 to 0.37. This was attributed to the expansion of the flow around the sharp corner of the outer shell at the throat. For the maximum expansion ratios, about 2.5, the integrated wall static pressure was higher for the rounded plug; this contradicts the peak thrust coefficients obtained with the sharp and rounded plugs. The peak thrust coefficient for the rounded plug at an expansion ratio of 2.5 was more reasonable as compared with the value obtained with a fixed-geometry nozzle in reference 1.

The peak thrust coefficient for the rounded plug was therefore believed to be correct, and the peak-thrust-coefficient value for the sharp plug was probably 1 to $1\frac{1}{2}$ percent high for an expansion-ratio setting of 2.50.

Although not presented, the pressure distribution along the vanes of the vaned nozzle was similar to that for the sharp- and rounded-plug nozzles except that the static pressure in the region of the throat was higher for the vaned nozzle.

Air-flow parameters. - The theoretical value of the air-flow parameter $W_a\sqrt{\theta}/A_5\delta$ for critical flow at the throat of a nozzle is 0.344 pounds per second per square inch. The ratio of the experimental values of air-flow parameter (fig. 8) to the theoretical value gave flow coefficients ranging from 0.945 to 0.983 for the sharp-plug nozzle, from 0.966 to 1.00 for the rounded-plug nozzle, and from 0.978 to 1.01 for the vaned nozzle. The vaned nozzle, then, had the highest over-all flow coefficients. The air-flow parameter obtained with the vaned nozzle at an expansion-ratio setting of 2.34 was in error, because the actual flow area at the throat of the nozzle could not be measured. As it turned out, the movable vanes had been so adjusted that the small circular arcs (see sketch (a)) at the opposite edges of the horizontal



Sketch (a)

flat surfaces of the fixed and movable blades, rather than the flat surfaces, were opposite each other at the minimum area; thus, the throat area was increased, as shown by dimension A in the sketch. The area between the flat surfaces, illustrated by dimension B, was used in calculating the air-flow parameter, because the exact area between the circular arcs could not be determined. This dimension between the vanes was so critical that, if the vanes had been so positioned that dimension A was increased by 0.012 of an inch, the flow coefficient would have been reduced 1 percent.

As pointed out previously, the peak thrust coefficients did not always occur at the design pressure ratio; they also occurred at pressure ratios higher than design. This indicated that the nozzles

were effectively operating at an expansion ratio higher than the physical expansion ratio of the nozzles. Generally, the peak thrust coefficient occurred at a nozzle pressure ratio higher than design for the low expansion-ratio setting and approached the design pressure ratio at the high expansion-ratio settings. The air-flow parameters, and consequently the flow coefficients, were lower at the low expansion ratios; the flow areas at the throats were therefore smallest in relation to the physical throats; as a result, the nozzles operated at an effectively higher expansion ratio and caused the peak thrust coefficients to occur at higher than design pressure ratios. The sharp-plug nozzle for an expansion-ratio setting of 2.27, which was next to the highest expansion-ratio setting, did not follow this trend. The air-flow parameter dropped to the lowest value of any expansion-ratio setting, and as a result the design pressure ratio was much lower than the pressure ratio at which the peak thrust coefficient occurred. This expansion-ratio setting of the sharp-plug nozzle was also shown herein to have a marked effect on the peak thrust coefficient. This discussion of the relation between air-flow parameter and the pressure ratio at which the peak thrust coefficient occurs applies mainly to the sharp-plug and the rounded-plug nozzles, because there was insufficient variation in the air-flow parameter of the vaned nozzle to show any marked trend except for the expansion-ratio setting of 2.34 which has been previously discussed.

Application of Results

The variable-throat convergent-divergent nozzles discussed herein are of the type which reduce the expansion ratio as the throat area is increased. In reference 4, it is pointed out that if this type of nozzle were applied to a supersonic turbojet interceptor, which was designed for a flight Mach number of 2 with afterburning, the nozzle efficiency for the nonafterburning subsonic-cruise condition would fall off considerably because of overexpansion of the nozzle. This general type of nozzle might, however, still be used on the supersonic turbojet aircraft if the outer shell were of the iris type so that the expansion ratio of the nozzle could also be controlled.

In the form investigated, these nozzles are applicable to ram-jet engines for some types of flight plan. In order to illustrate the application of the type nozzle investigated to a ram-jet flight plan, the following assumptions were made: (a) the ram-jet-powered vehicle is air launched at an altitude of 35,000 feet and is boosted to a Mach number of 2.13, and (b) the vehicle is accelerated to a Mach number of 3.0. Variations of nozzle geometry and obtainable thrust coefficients over the range of Mach numbers covered during the period of acceleration are shown in figure 9. The ratio of nozzle-throat area to combustion-chamber area required to maintain critical diffuser operation for the ram jet at stoichiometric fuel-air ratio is shown in figure 9(a). The

ratio of nozzle-throat area to combustion-chamber area decreases from a value of 0.55 at a Mach number of 2.13 to 0.45 at a Mach number of 3.0.

Nozzle expansion ratios for nozzles with three different geometrical characteristics are shown in figure 9(b). The nozzle-throat-area variation shown in figure 9(a) was assumed for the three cases of expansion-ratio variation shown in figure 9(b). The ideal isentropic expansion ratio (complete expansion of the flow) for the nozzle pressure ratio obtained at each flight Mach number is shown by the solid curve. The geometrical characteristics of the rounded-plug nozzle were used to obtain the other two curves shown in figure 9(b). The dashed curve shows the variation in expansion ratio which results if the ideal expansion ratio at a Mach number of 2.55 is matched. The curve composed of alternate dots and dashes shows the variation in expansion ratio which results if the ideal expansion ratio at a Mach number of 2.13 is matched. The actual variation in expansion ratio for these last two cases is, of course, a function of the throat-area variation and the geometry of the nozzle shell and plug.

The obtainable nozzle thrust coefficients for the nozzles with expansion-ratio variations shown in figure 9(b) are shown in figure 9(c). The performance characteristics of the rounded-plug nozzle were used to obtain the thrust coefficients shown. The rounded-plug-nozzle data were extended to higher nozzle pressure ratios than those investigated by the method described in reference 5 in order to obtain parts of some of the thrust coefficient curves shown in figure 9(c). The thrust coefficient for the nozzle with the ideal-isentropic-expansion-ratio variation is shown by the solid curve. The thrust coefficient decreased from a value of 0.96 at a flight Mach number of 2.13 to 0.95 at a flight Mach number of 2.66. Nozzle thrust coefficients at flight Mach numbers greater than 2.66 could not be shown because the corresponding ideal isentropic expansion ratios were beyond the range of expansion ratios covered by the experimental investigation.

The thrust coefficient for the nozzle which matches the ideal isentropic expansion ratio only at a flight Mach number of 2.55 is shown by the dashed curve. At a Mach number of 2.55, the thrust coefficient is 0.95 (equal to that for the ideal-isentropic-expansion-ratio nozzle). As the Mach number decreases below 2.55, the thrust coefficient falls below that for the ideal-isentropic-expansion-ratio nozzle because of overexpansion. At a Mach number of 2.13, the thrust coefficient decreased to a value of 0.92 which is 4 percent below that for the ideal isentropic expansion-ratio nozzle. At flight Mach numbers greater than 2.55, the thrust coefficient drops off very slowly to a value of 0.944 at a flight Mach number of 3.0.

The thrust coefficient for the nozzle which matches the ideal isentropic expansion ratio at a flight Mach number of 2.13 is shown by the

alternate dash-dot curve. The thrust coefficient for this nozzle decreases from a value of 0.96 at a flight Mach number of 2.13 to 0.94 at a flight Mach number of 3.0. Although this nozzle is physically underexpanded for all Mach numbers greater than 2.13, the thrust coefficients are very close to those for the nozzle with the ideal isentropic expansion ratio and even slightly higher for Mach numbers from 2.25 to 2.5. The fact that the thrust coefficient for a nozzle which is physically underexpanded can be equal to or greater than that for a nozzle with an ideal isentropic expansion ratio exists because, within the range of nozzle pressure ratios involved, the locus of maximum thrust coefficients (see fig. 6(b)) decreases with increasing nozzle pressure ratio at approximately the same rate as the thrust coefficient for an underexpanded nozzle. This characteristic is further illustrated by the alternate dash-dot-dot curve in figure 9(c) which shows the maximum thrust coefficient obtainable at the nozzle pressure ratio corresponding to each Mach number. A nozzle giving this performance has both variable throat and exit and at each Mach number operates at an expansion ratio which is lower than the ideal isentropic value corresponding to the nozzle pressure ratio. The thrust coefficients for such a nozzle decrease from a value of 0.974 at a Mach number of 2.13 to 0.95 at a Mach number of 2.66.

CONCLUDING REMARKS

An internal flow investigation showed small variations between the peak thrust coefficients of three variable-throat convergent-divergent nozzles. The peak thrust coefficients for these nozzles varied from 0.945 to 0.975 over a range of nozzle pressure ratios from 6 to 16. These thrust coefficients approached or equalled those previously obtained with several fixed-geometry convergent-divergent nozzles. There was little gain in the peak thrust coefficient of a variable-throat plug-type convergent-divergent nozzle when the sharp corner of a conical center plug was rounded.

The nozzles investigated were of the type best suited for use with ram-jet missiles designed to operate over a wide range of flight Mach numbers. Application of the data obtained with the rounded-plug nozzle to a typical flight plan of a ram-jet missile showed that a thrust coefficient of approximately 0.95 was possible over a range of flight Mach numbers from 2.13 to 3.0 by proper matching of the nozzle to the required nozzle operating schedule. With the performance characteristics of the nozzles investigated, this maximum thrust coefficient was obtained by matching the nozzle expansion ratio to the flight plan at the minimum flight Mach number and allowing the nozzle to operate underexpanded at the higher flight Mach numbers.

Lewis Flight Propulsion Laboratory
National Advisory Committee for Aeronautics
Cleveland, Ohio, March 12, 1953

APPENDIX - SYMBOLS AND METHODS OF CALCULATION

Symbols

The following symbols are used in this report:

A	outside area, sq ft
A'	inside area, sq ft
A_s	outside area of mounting pipe, sq ft
C_T	thrust coefficient
C_X	thermal-expansion coefficient, ratio of area when hot to area when cold
F	thrust, lb
F_d	balanced-air-pressure-diaphragm force, lb
g	acceleration due to gravity, 32.2 ft/sec^2
M	Mach number
m	mass flow, slugs/sec
P	total pressure, lb/sq ft
p	static pressure, lb/sq ft
p_{bm}	integrated static pressure acting on outside of bellmouth inlet to station 2, lb/sq ft
p_d	integrated static pressure acting on outside of diffuser, lb/sq ft
R	gas constant, 53.3 ft-lb/(lb)($^\circ$R) for air
T	total temperature, $^\circ$R
V	velocity, ft/sec
W_a	air flow, lb/sec
γ	ratio of specific heats

δ ratio of total pressure at nozzle inlet to absolute pressure at NACA standard sea-level conditions

θ ratio of total temperature at nozzle inlet to absolute temperature at NACA standard sea-level conditions

Subscripts:

e nozzle exit

i ideal

j jet

0 exhaust

1 mounting pipe inlet, modified inlet pipe

2 diffuser inlet

3 mounting pipe inlet, original inlet pipe

4 nozzle inlet

5 nozzle throat

Methods of Calculation

Air flow. - The nozzle air flow for the original test chamber was computed as

$$W_a = \frac{p_4 A_4 C_X}{\sqrt{RT_4}} \sqrt{\frac{2g\gamma}{\gamma-1}\left[\left(\frac{P_4}{p_4}\right)^{\frac{\gamma-1}{\gamma}} - 1\right]\left(\frac{P_4}{p_4}\right)^{\frac{\gamma-1}{\gamma}}}$$

and for the modified test chamber as

$$W_a = \frac{p_2 A_2 C_X}{\sqrt{RT_4}} \sqrt{\frac{2g\gamma}{\gamma-1}\left[\left(\frac{P_2}{p_2}\right)^{\frac{\gamma-1}{\gamma}} - 1\right]\left(\frac{P_2}{p_2}\right)^{\frac{\gamma-1}{\gamma}}}$$

The value of γ was assumed to be 1.4, and values of the thermal-expansion coefficient C_X of the areas at the respective stations were obtained from the thermal-expansion coefficient for the material and the temperature of the material. The material temperature was assumed to be the same as the temperature of the air flowing through the respective station.

Thrust. - The jet thrust was defined as

$$F_j = m_2 V_e + A_e(p_e - p_0)$$

The actual jet thrust was calculated for the original inlet pipe by use of the following equation:

$$F_j = \frac{W_a V_3}{g} + C_X A_s(p_3 - p_0) - F_d$$

and for the modified inlet pipe from

$$F_j = \frac{W_a V_1}{g} + p_1 A_1 C_X + p_d(A_s - A_2')C_X - p_{bm}(A_1 - A_2')C_X - p_0 A_s - F_d$$

where F_d was obtained from balanced-air-pressure-diaphragm measurements. The value of p_1 and V_1 were computed by one-dimensional flow relations from the total and static pressures measured at station 2 and the total temperature measured at station 4. This method was checked by actual preliminary pressure measurements at station 1 and found to be accurate.

The ideally available thrust was calculated as

$$F_i = W_a \sqrt{\frac{2R}{g} \frac{\gamma}{\gamma-1} T_4 \left[1 - \left(\frac{p_0}{P_4}\right)^{\frac{\gamma-1}{\gamma}}\right]}$$

Thrust coefficient. - The thrust coefficient is defined as the ratio of actual to theoretical jet thrust

$$C_T = \frac{F_j}{F_i}$$

REFERENCES

1. Krull, H. George, and Steffen, Fred W.: Performance Characteristics of One Convergent and Three Convergent-Divergent Nozzles. NACA RM E52H12, 1952.

2. Reshotko, Eli: Preliminary Investigation of a Perforated Axially Symmetric Nozzle for Varying Nozzle Pressure Ratios. NACA RM E52J27, 1953.

3. Schairer, G.: Performance Characteristics of Jet Nozzles. Doc. No. D-12054, Boeing Airplane Co., Seattle (Wash.), July 25, 1951.

4. Fleming, William A.: Internal Performance of Several Types of Jet-Exit Configuration for Supersonic Turbojet Aircraft. NACA RM E52K04, 1953.

5. Povolny, John H.: Use of Choked Nozzle Technique and Exhaust Jet Diffuser for Extending Operable Range of Jet-Engine Research Facilities. NACA E52E12, 1952.

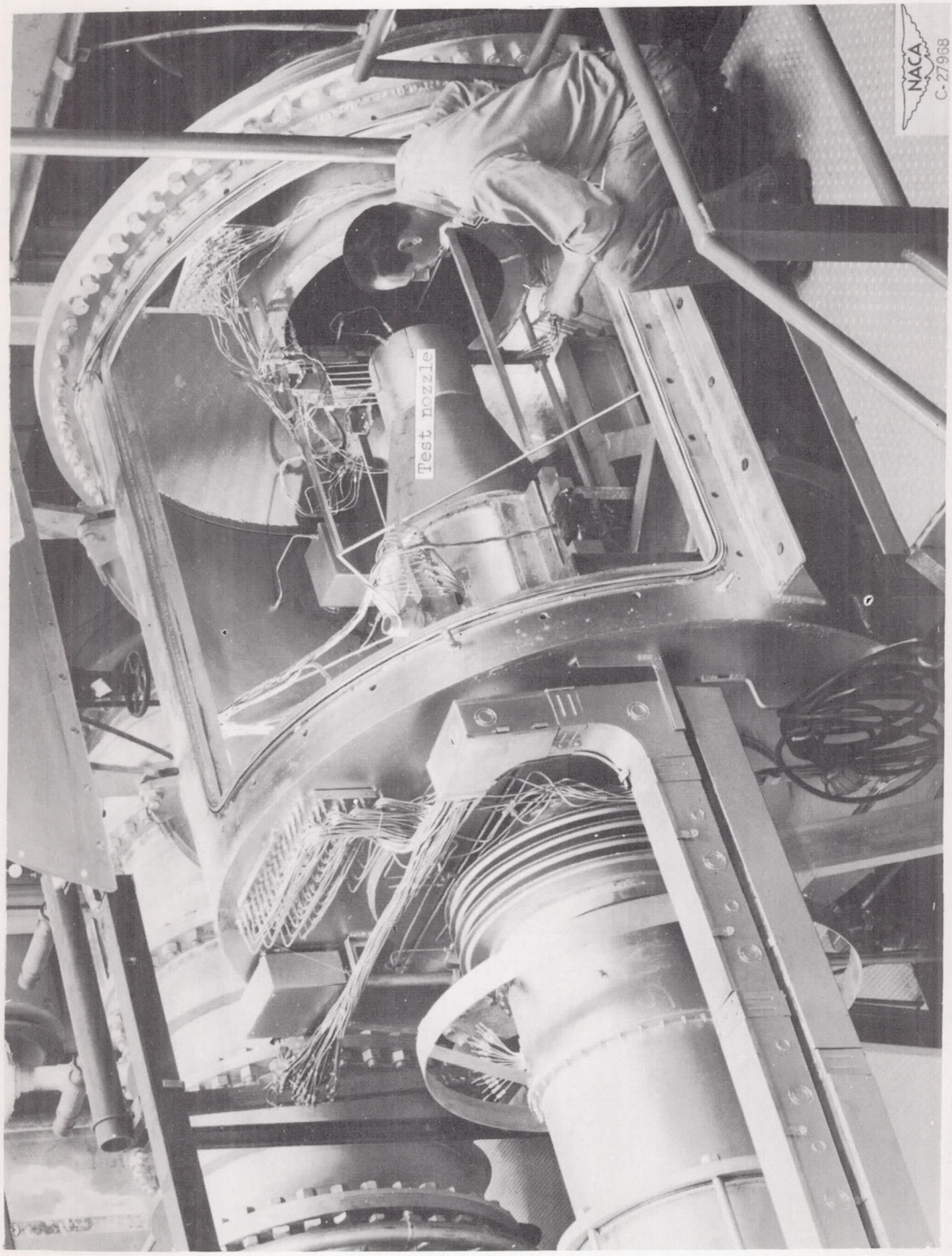
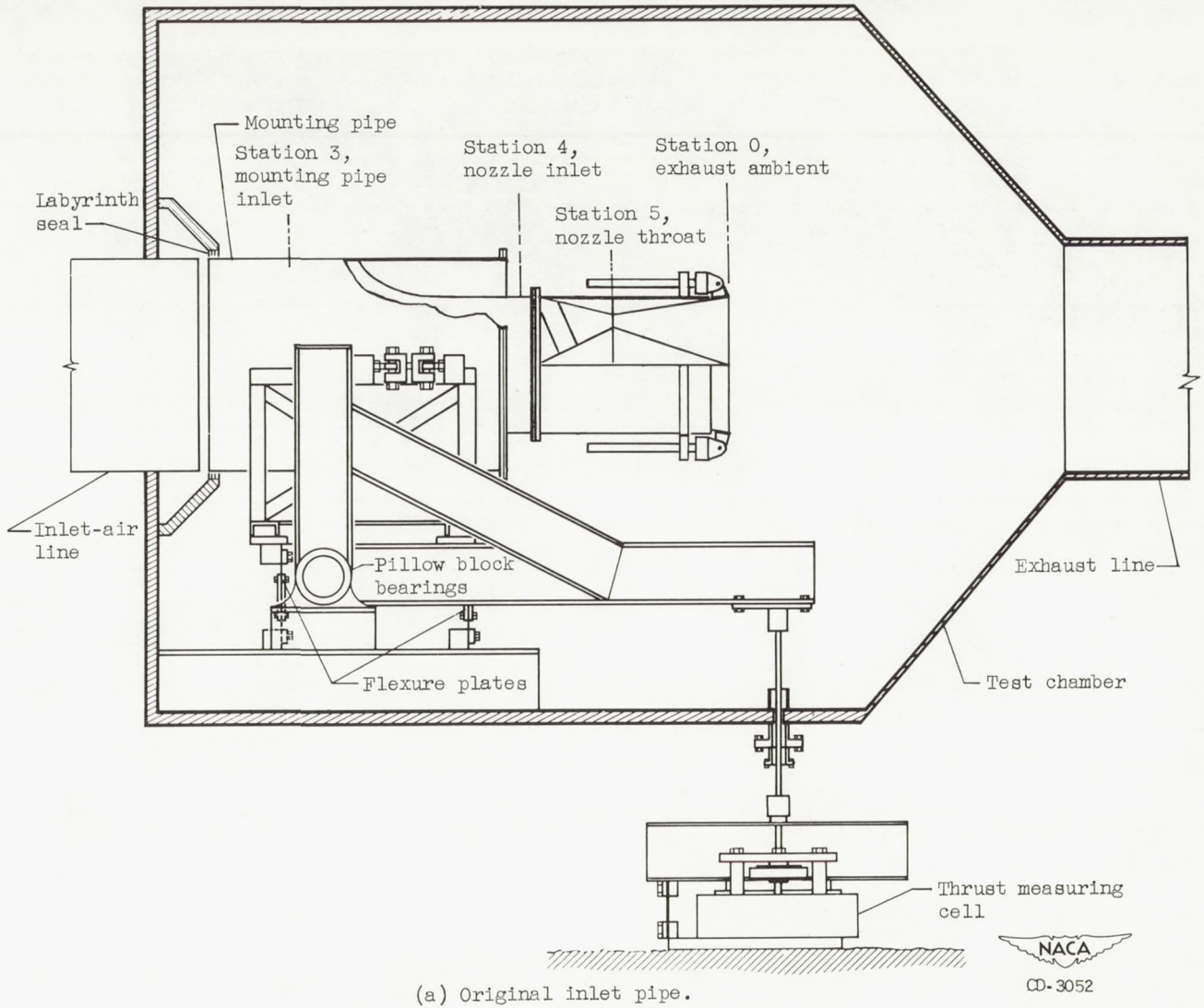
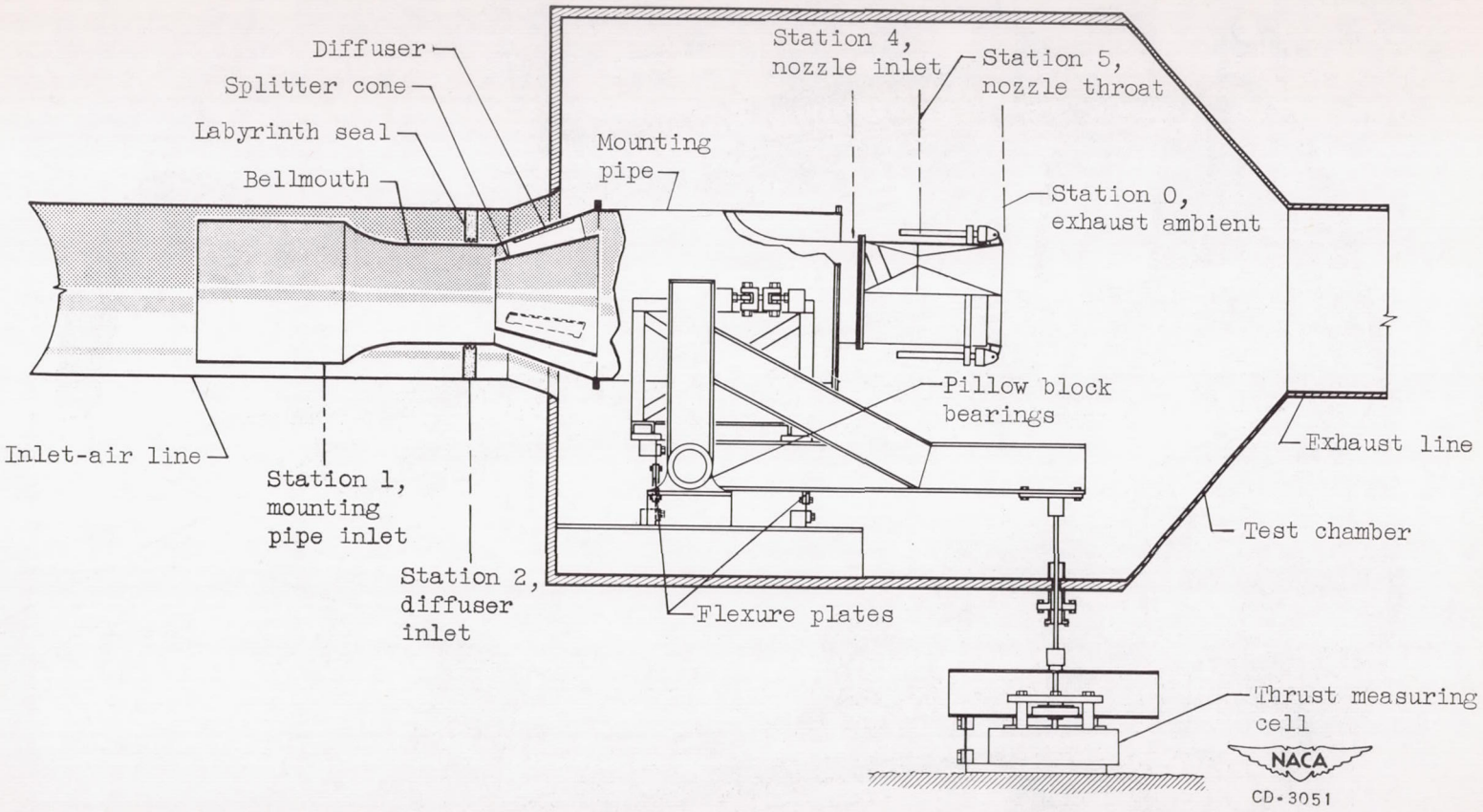


Figure 1. - Installation of nozzle in test chamber.



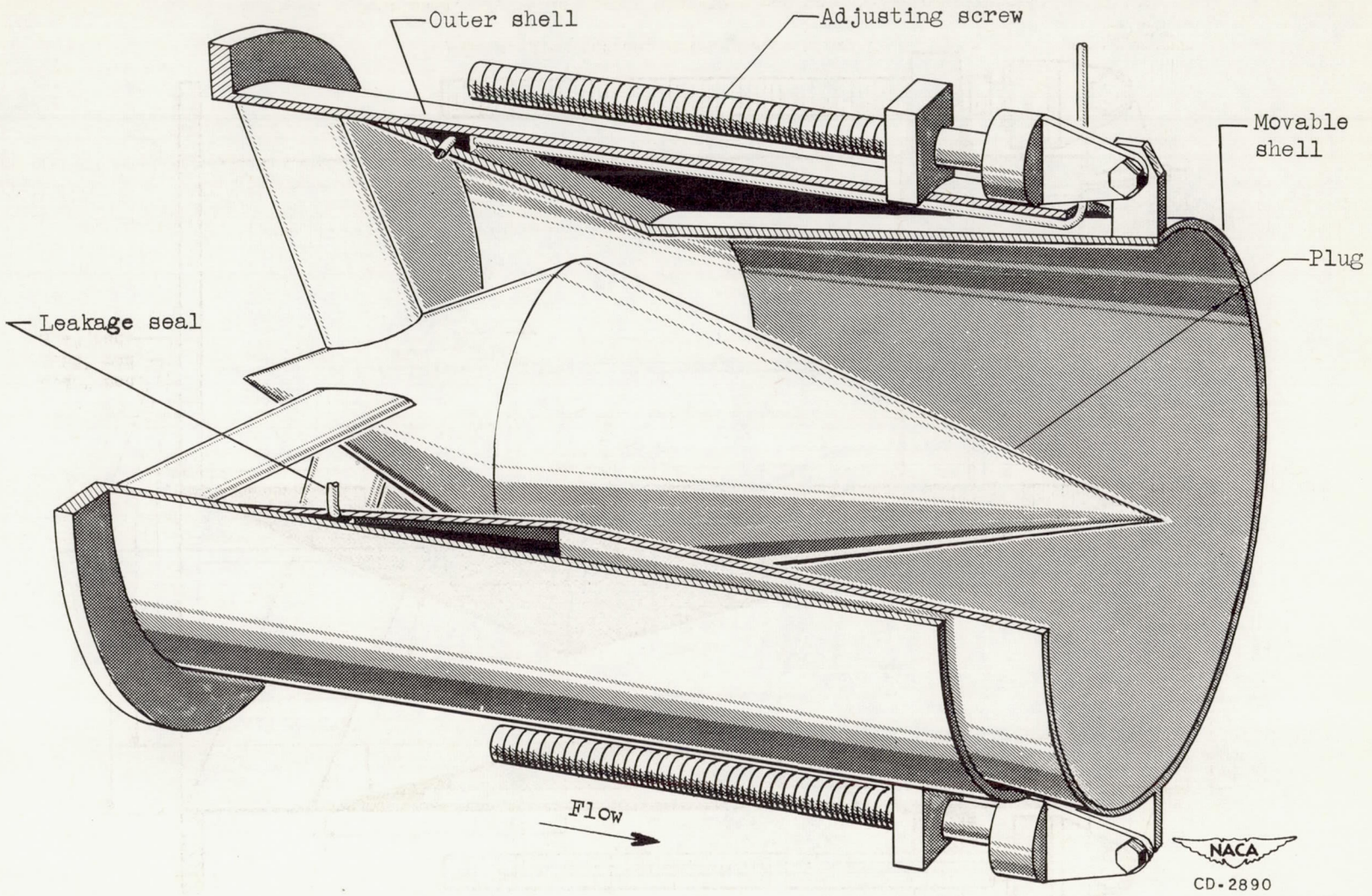
(a) Original inlet pipe.

Figure 2. - Schematic drawing of nozzle in test chamber.



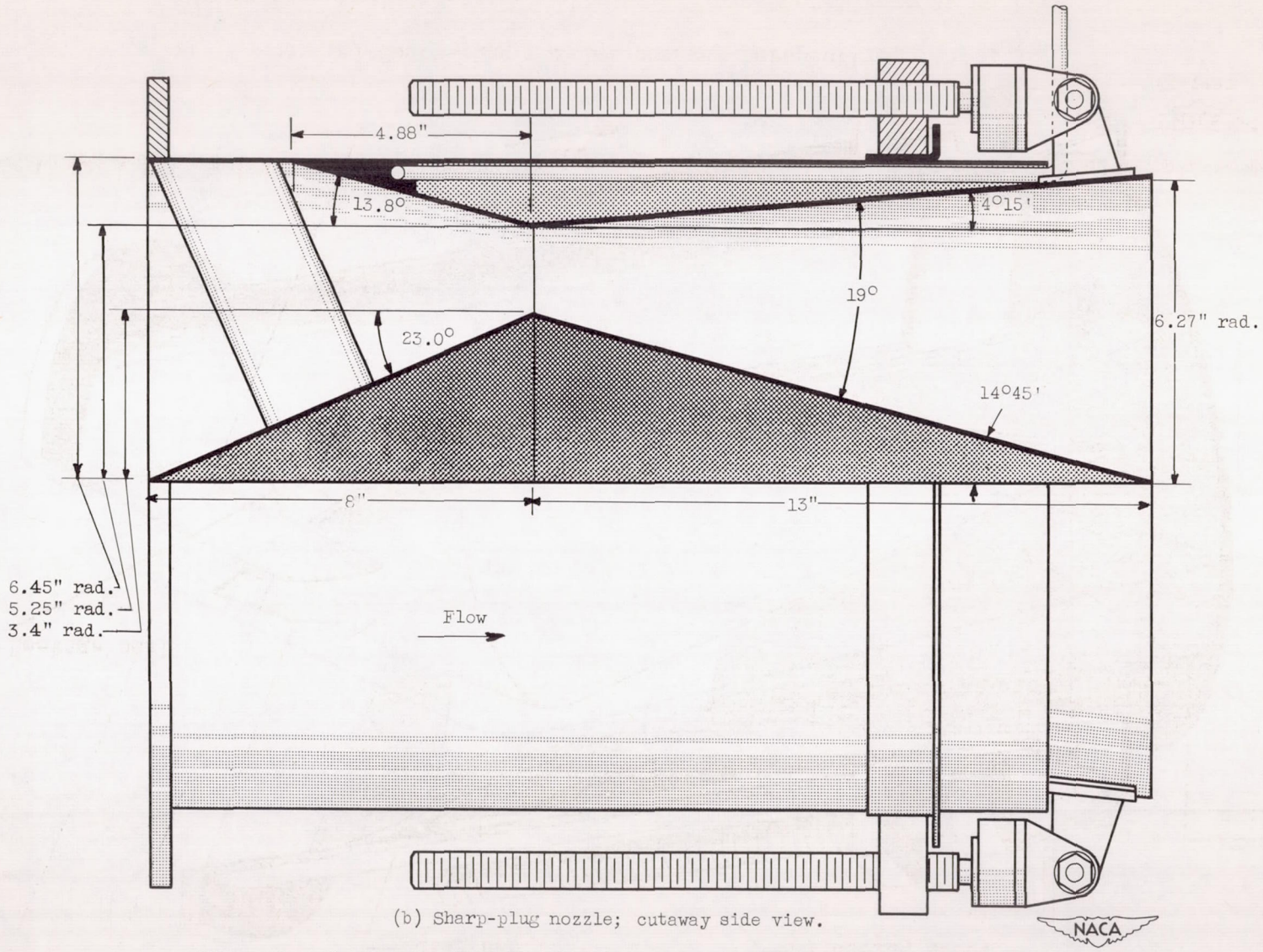
(b) Modified inlet pipe

Figure 2. - Concluded. Schematic drawing of nozzle in test chamber.



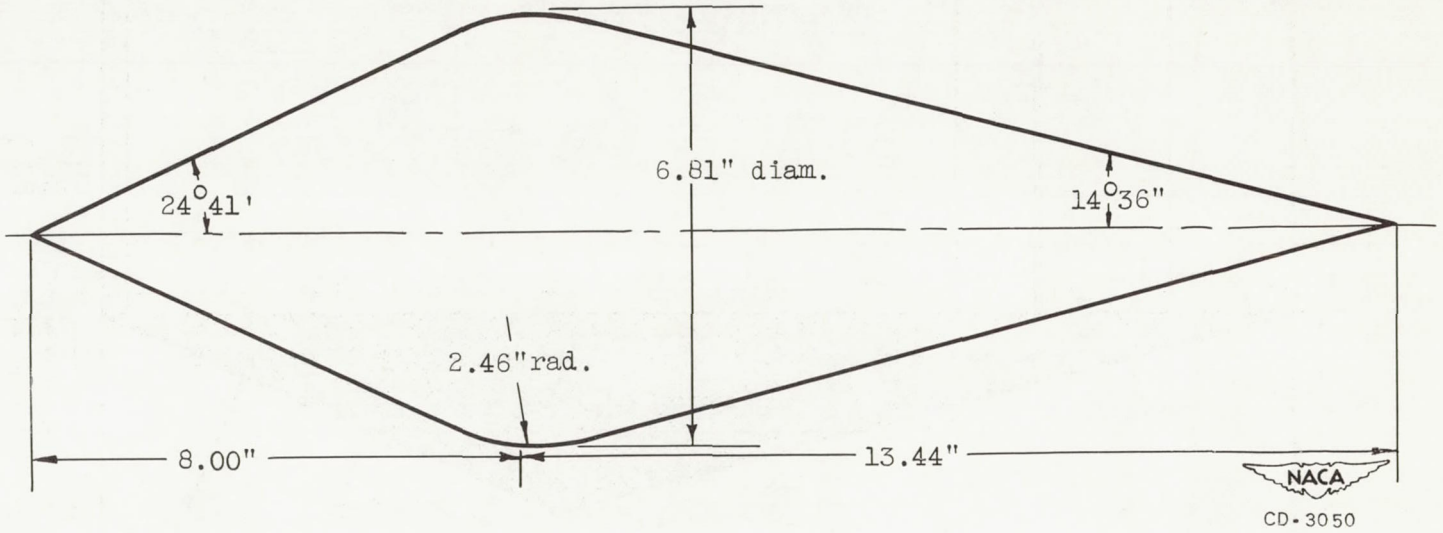
(a) Sharp-plug nozzle; cutaway perspective.

Figure 3. - Variable-throat plug-type convergent-divergent nozzle.



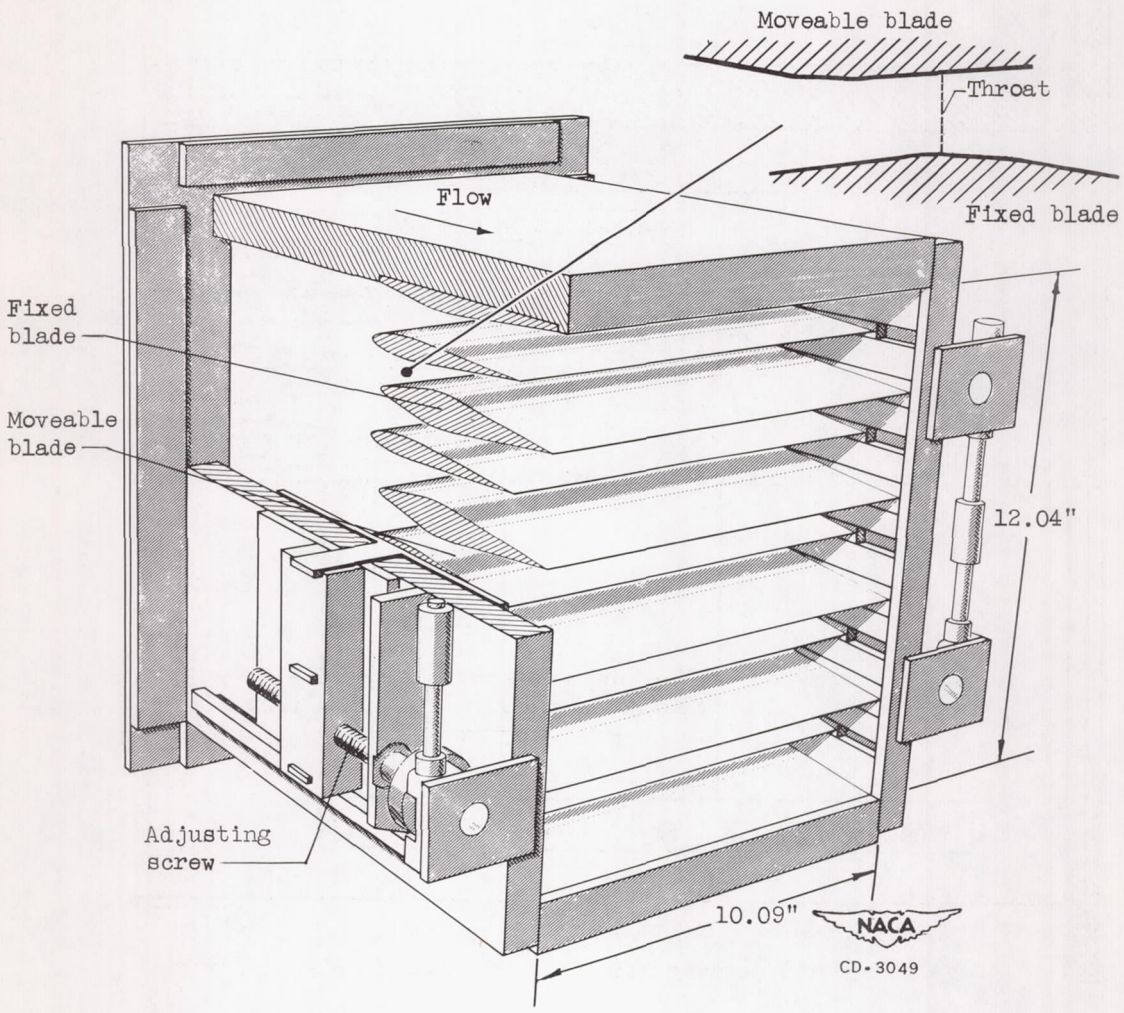
(b) Sharp-plug nozzle; cutaway side view.

Figure 3. - Continued. Variable-throat plug-type convergent-divergent nozzle. CD-2892



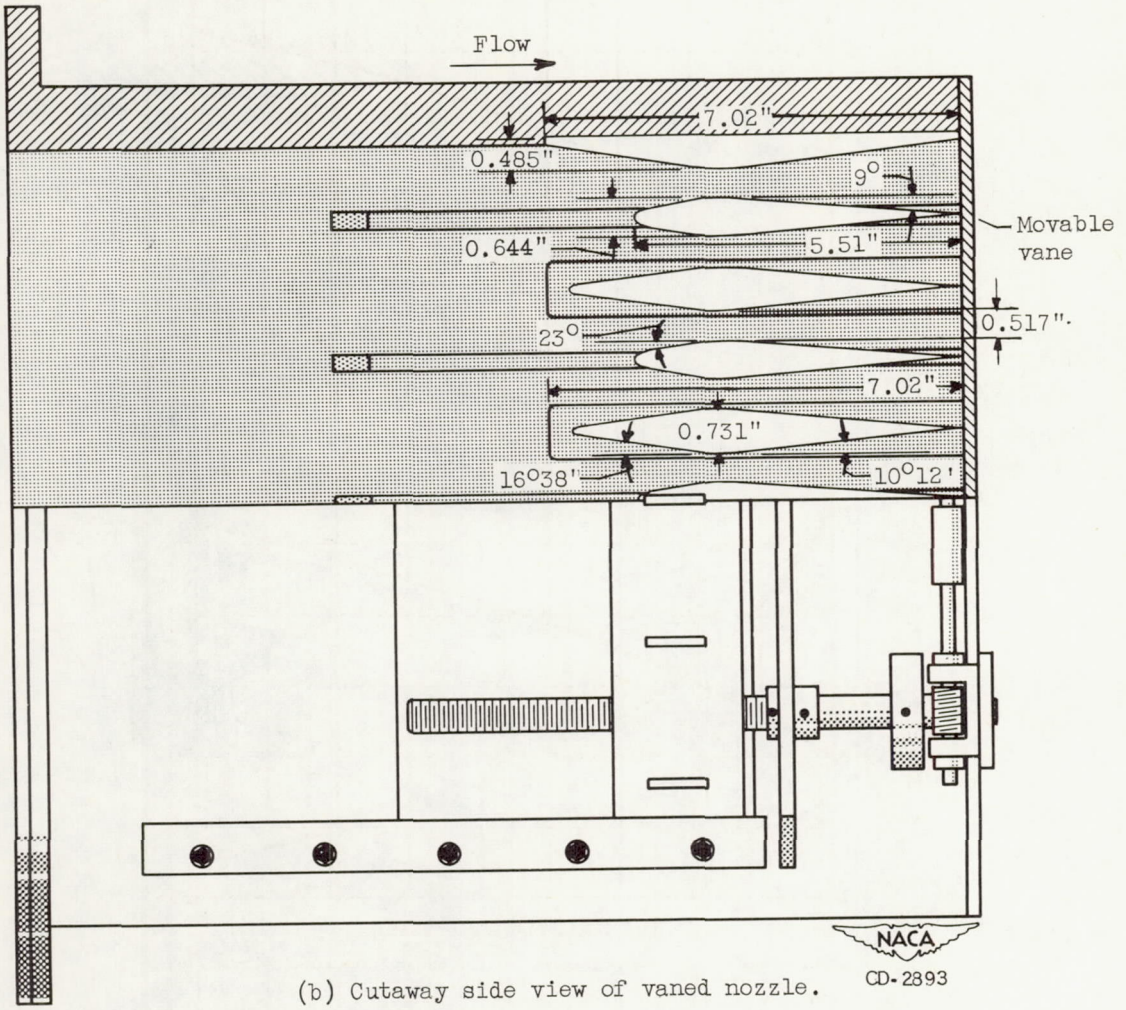
(c) Rounded plug.

Figure 3. - Concluded. Variable-throat plug-type convergent-divergent nozzle.



(a) Cutaway perspective.

Figure 4. - Variable-throat vaned-type convergent-divergent nozzle.



(b) Cutaway side view of vaned nozzle.

Figure 4. - Concluded. Variable-throat vaned-type convergent-divergent nozzle.

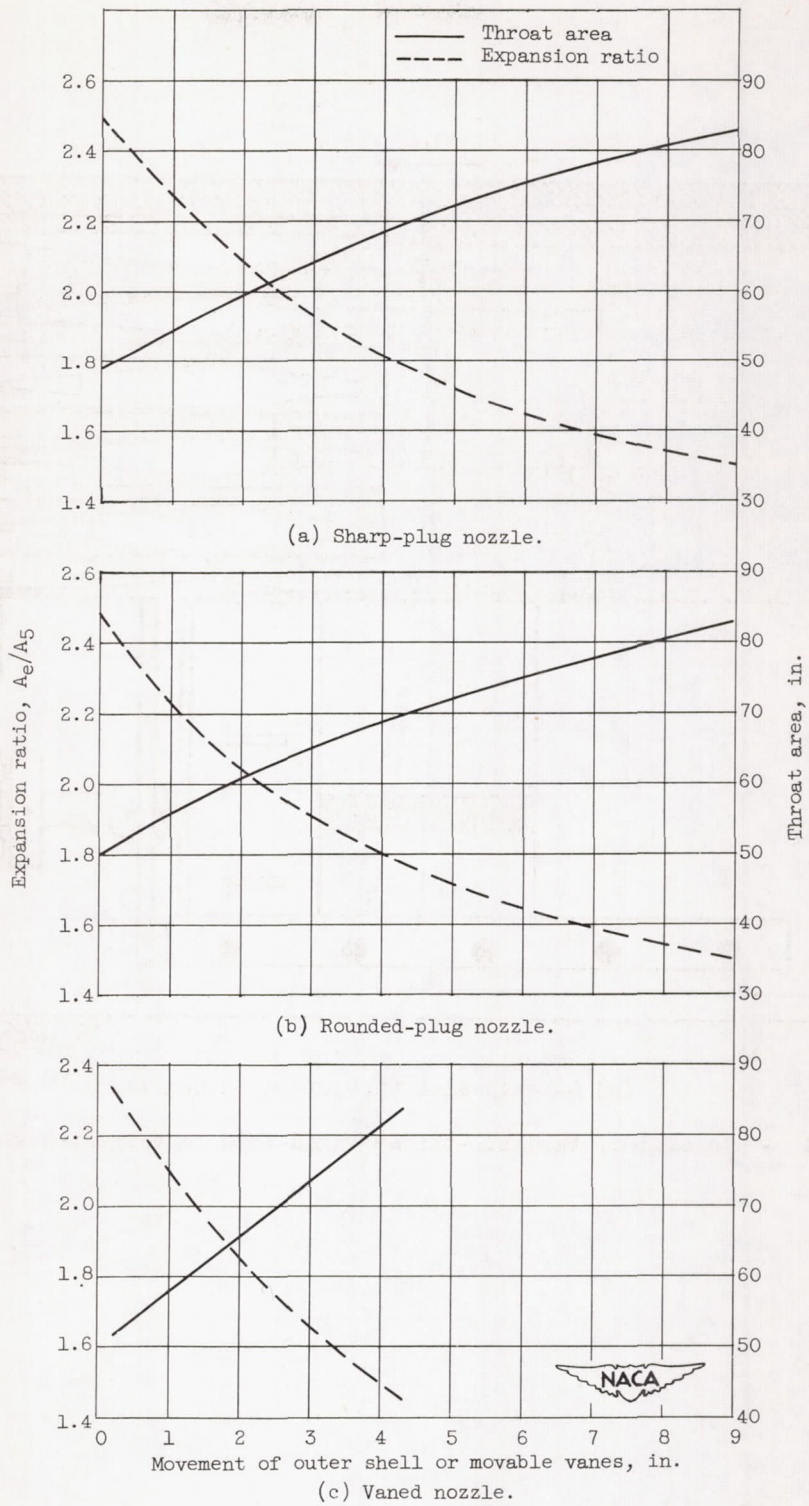
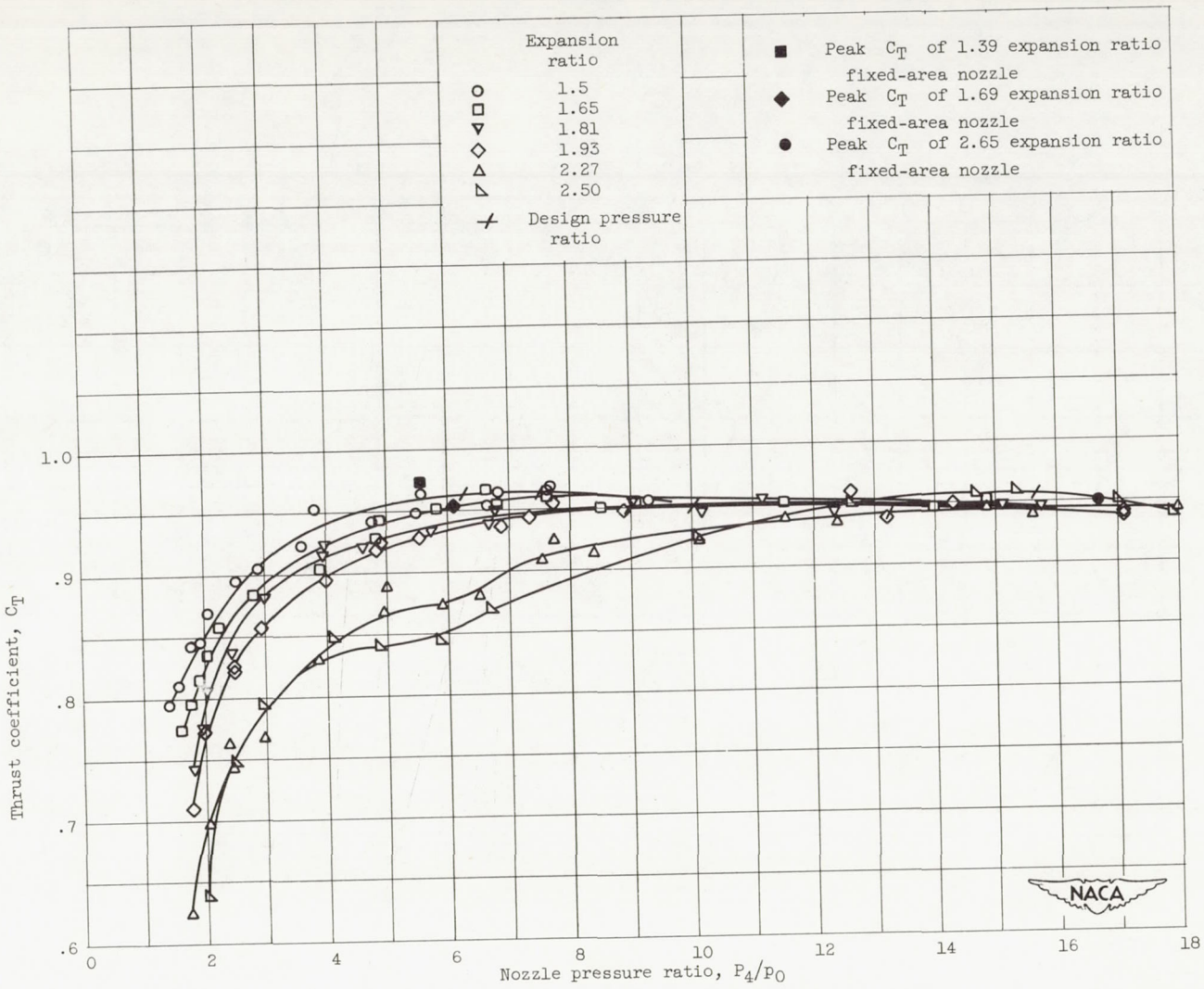
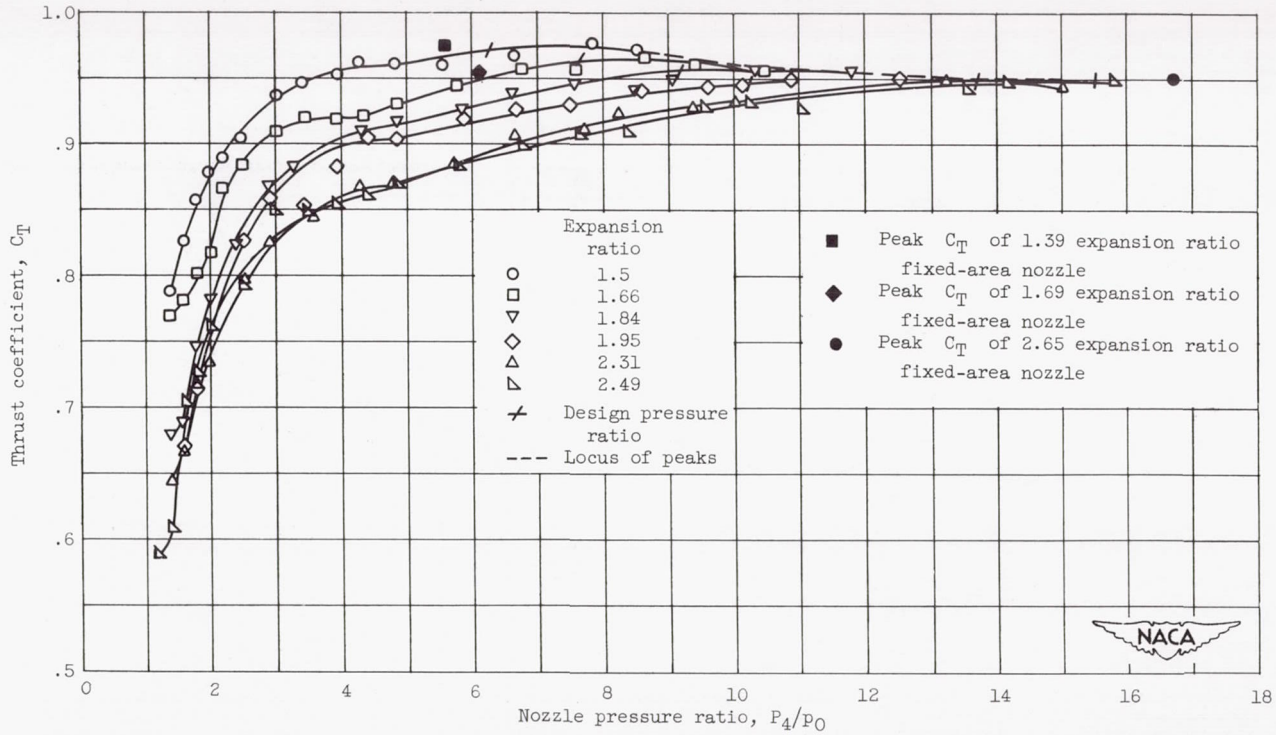


Figure 5. - Variation of expansion ratio with throat area for three variable-throat convergent-divergent nozzles.



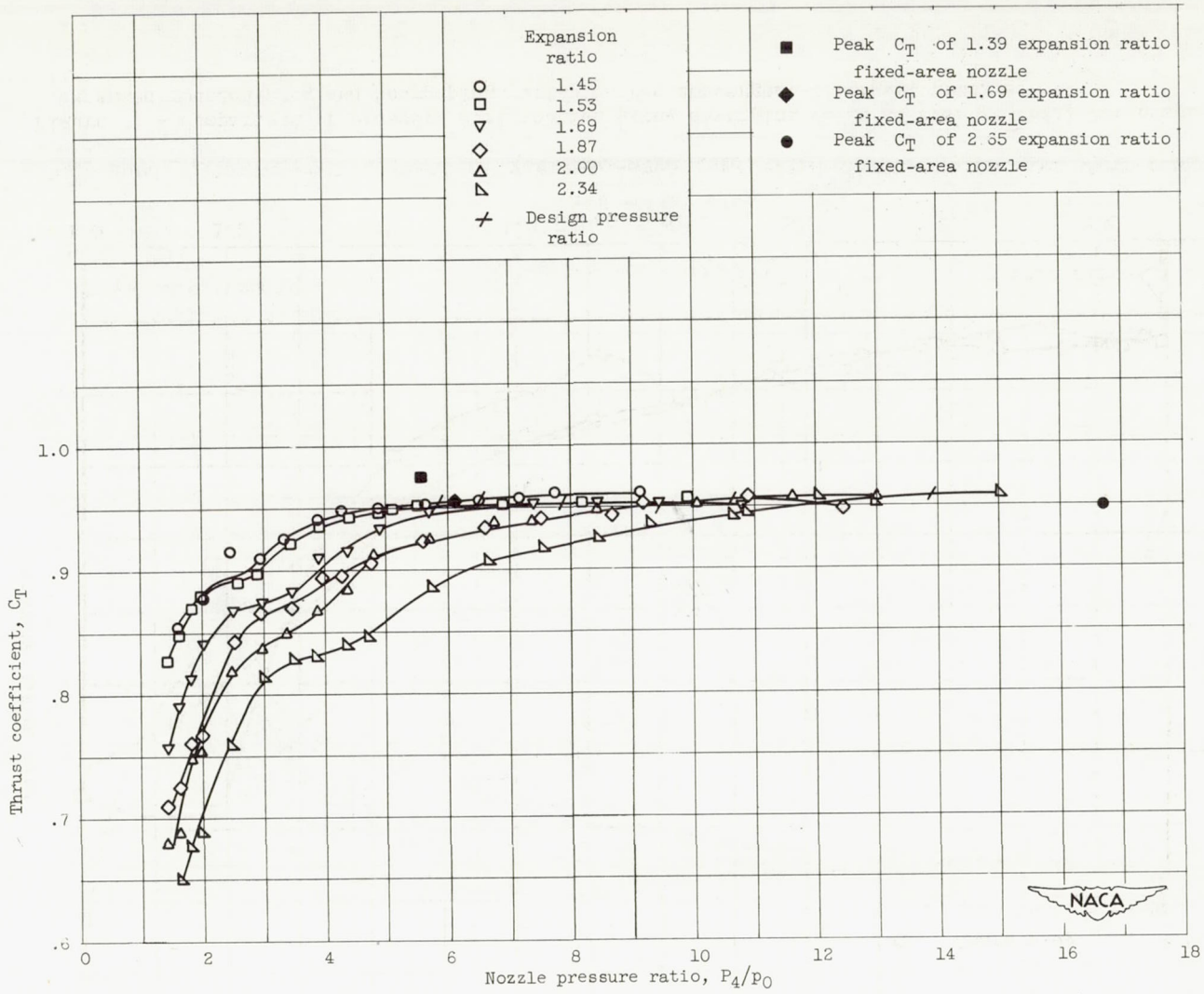
(a) Sharp-plug nozzle.

Figure 6. - Thrust coefficients of variable-area convergent-divergent nozzles over range of nozzle pressure ratios.



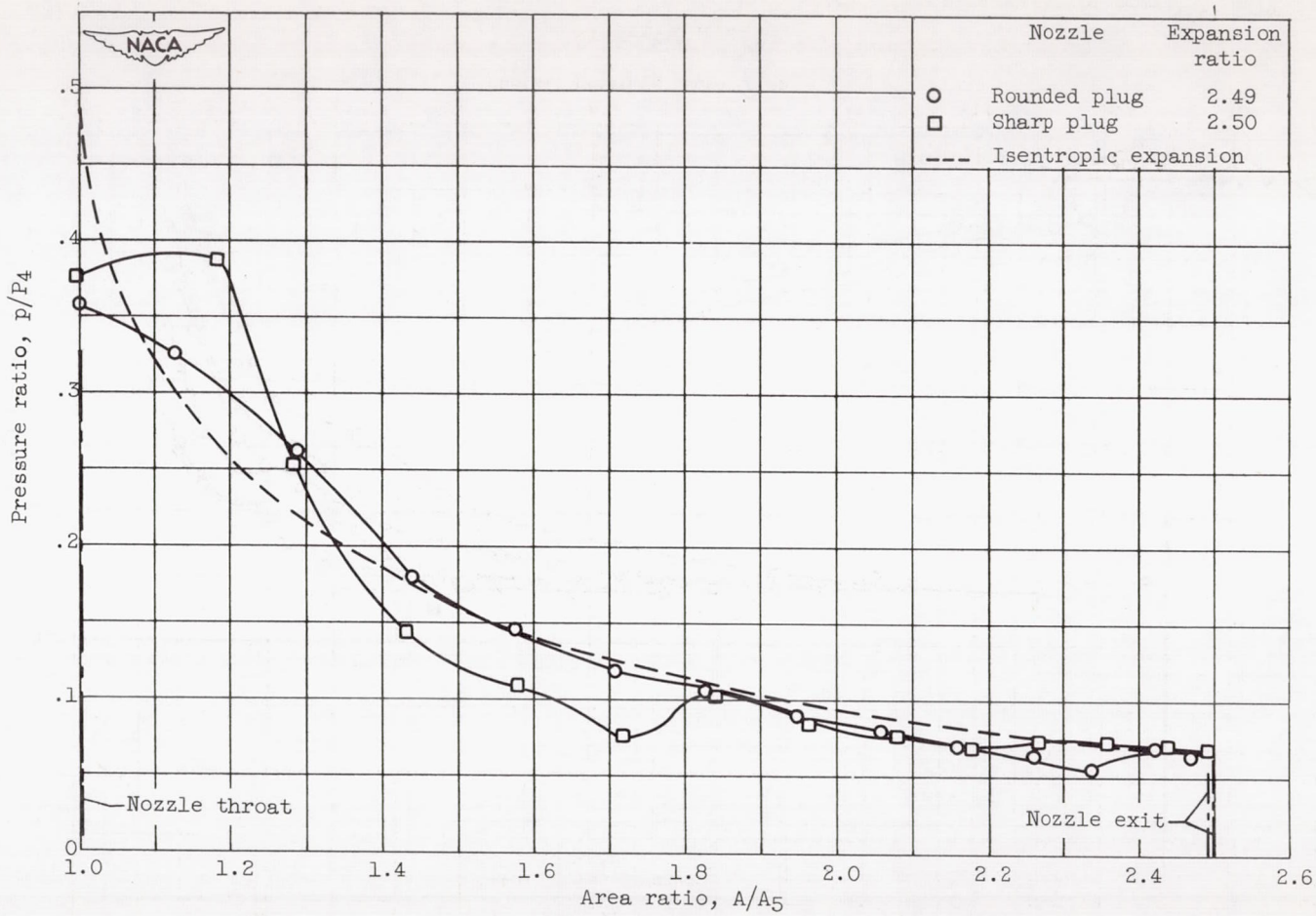
(b) Rounded-plug nozzle.

Figure 6. - Continued. Thrust coefficients of variable-area convergent-divergent nozzles over range of nozzle pressure ratios.



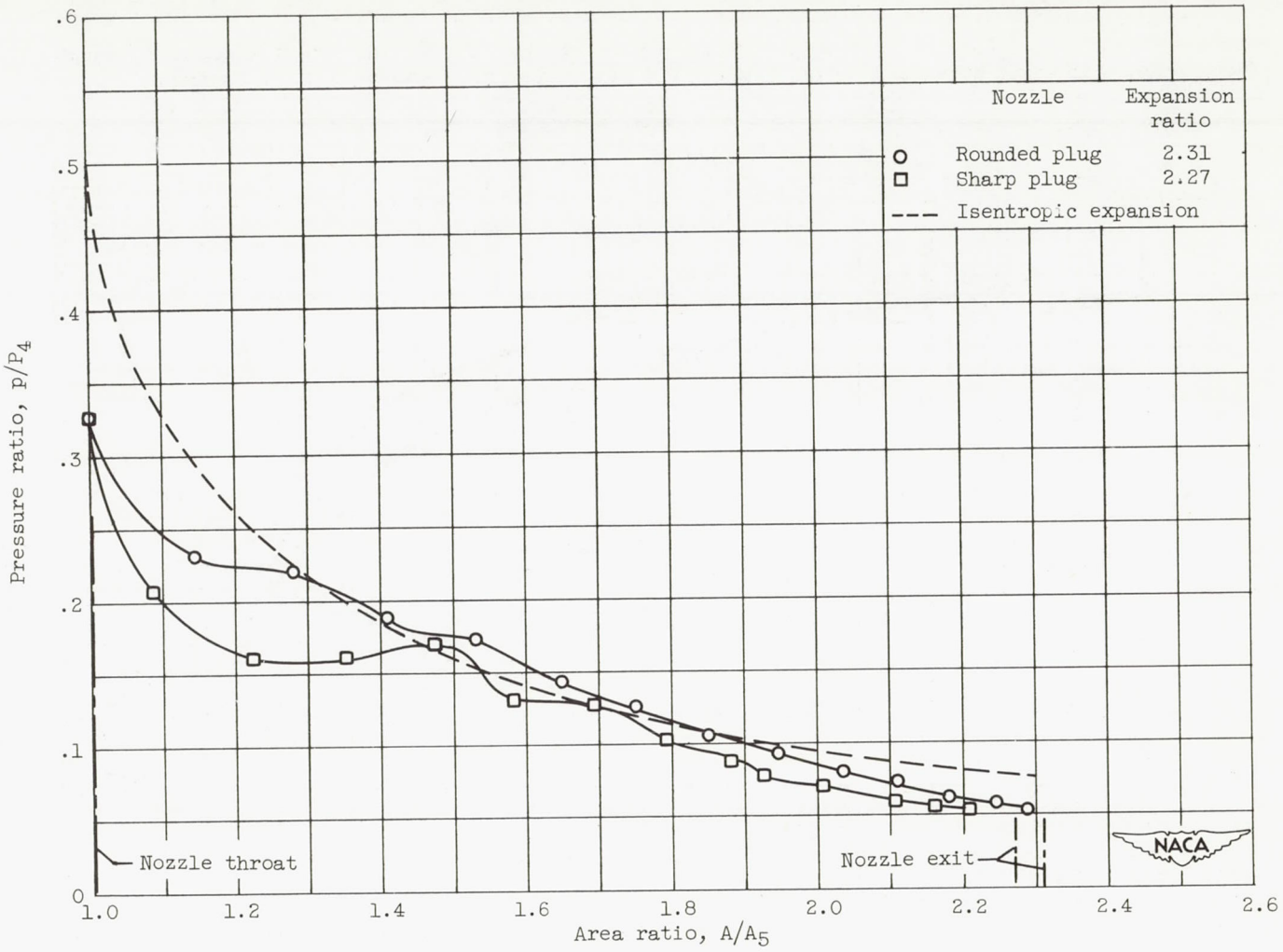
(c) Vaned nozzle.

Figure 6. - Concluded. Thrust coefficients of variable-area convergent-divergent nozzles over range of nozzle pressure ratios.



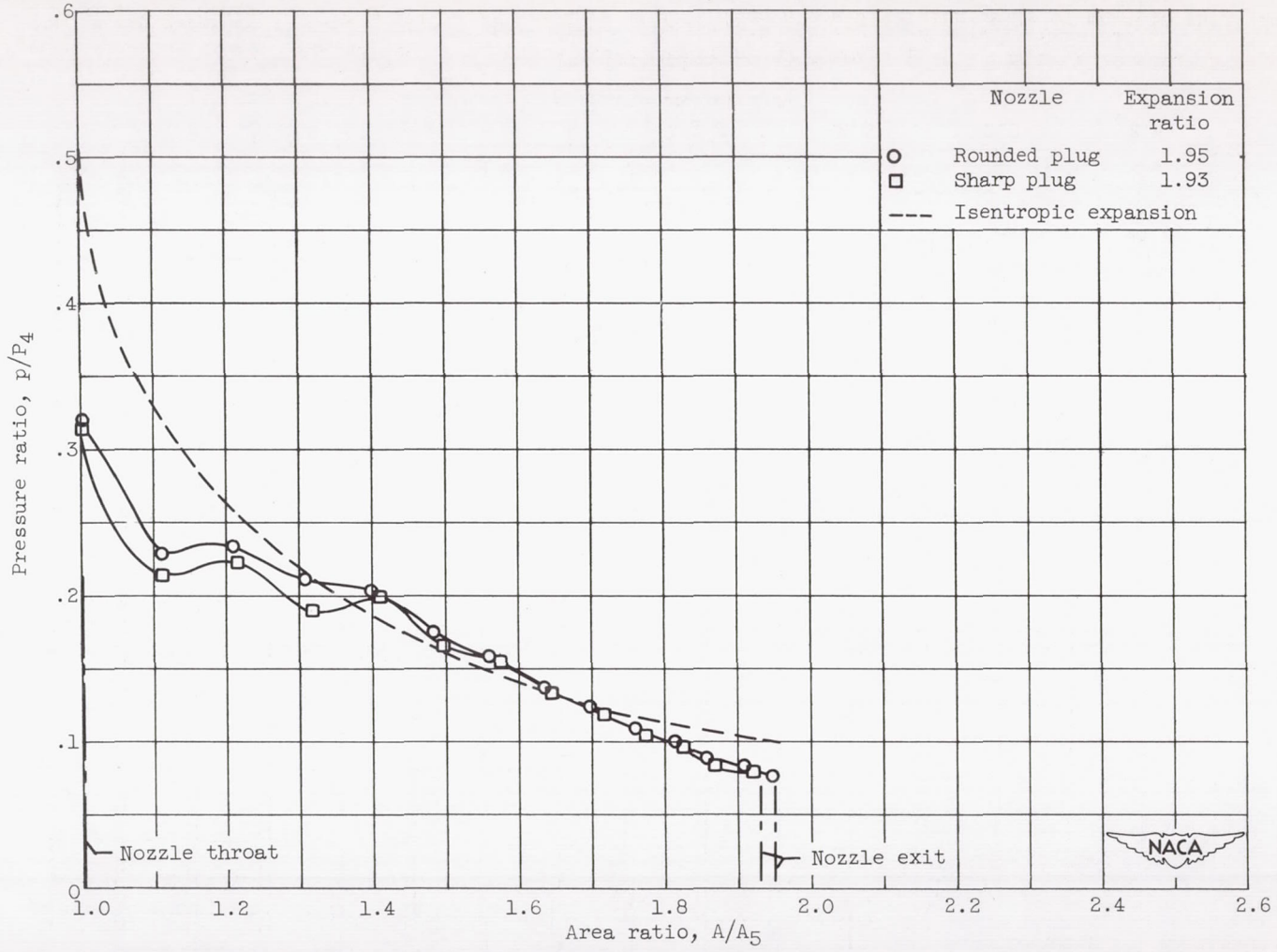
(a) Expansion ratio, 2.5.

Figure 7. - Comparison of pressure distribution along diverging walls of movable shell for completely expanded rounded-plug and sharp-plug variable-area convergent-divergent nozzles.



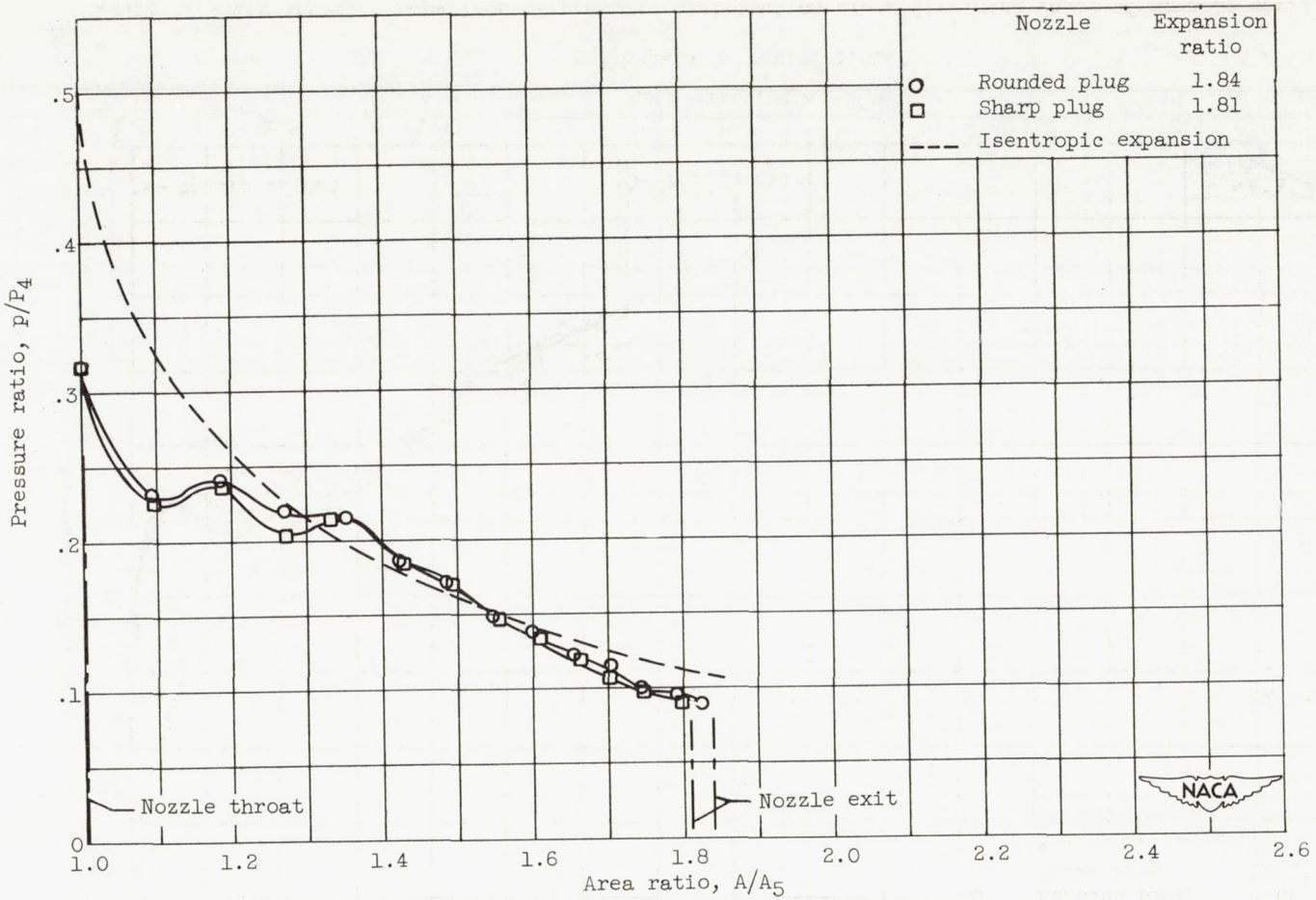
(b) Expansion ratio, 2.3.

Figure 7. - Continued. Comparison of pressure distribution along diverging walls of movable shell for completely expanded rounded-plug and sharp-plug variable-area convergent-divergent nozzles.



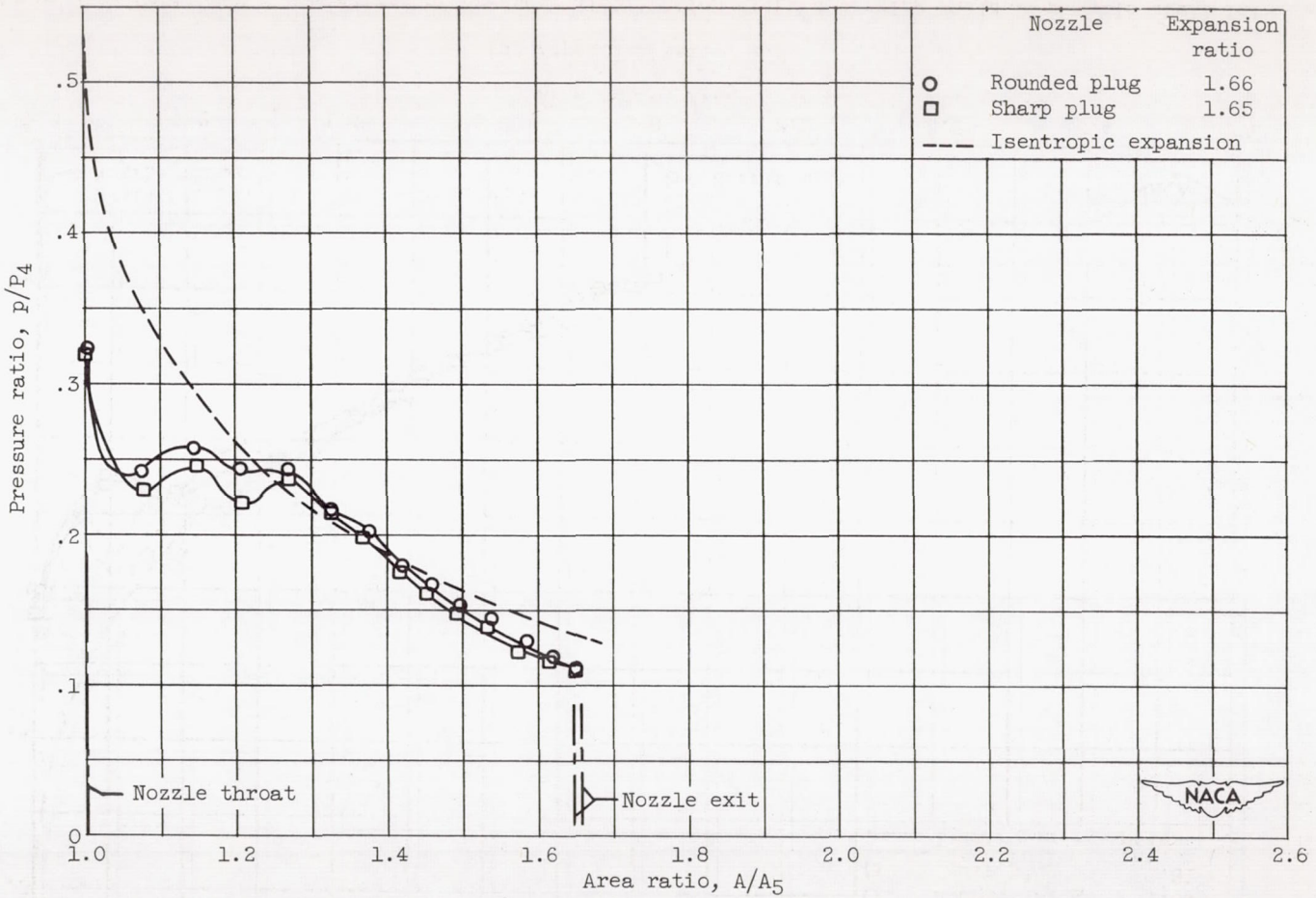
(c) Expansion ratio, 1.9.

Figure 7. - Continued. Comparison of pressure distribution along diverging walls of movable shell for completely expanded rounded-plug and sharp-plug variable-area convergent-divergent nozzles.



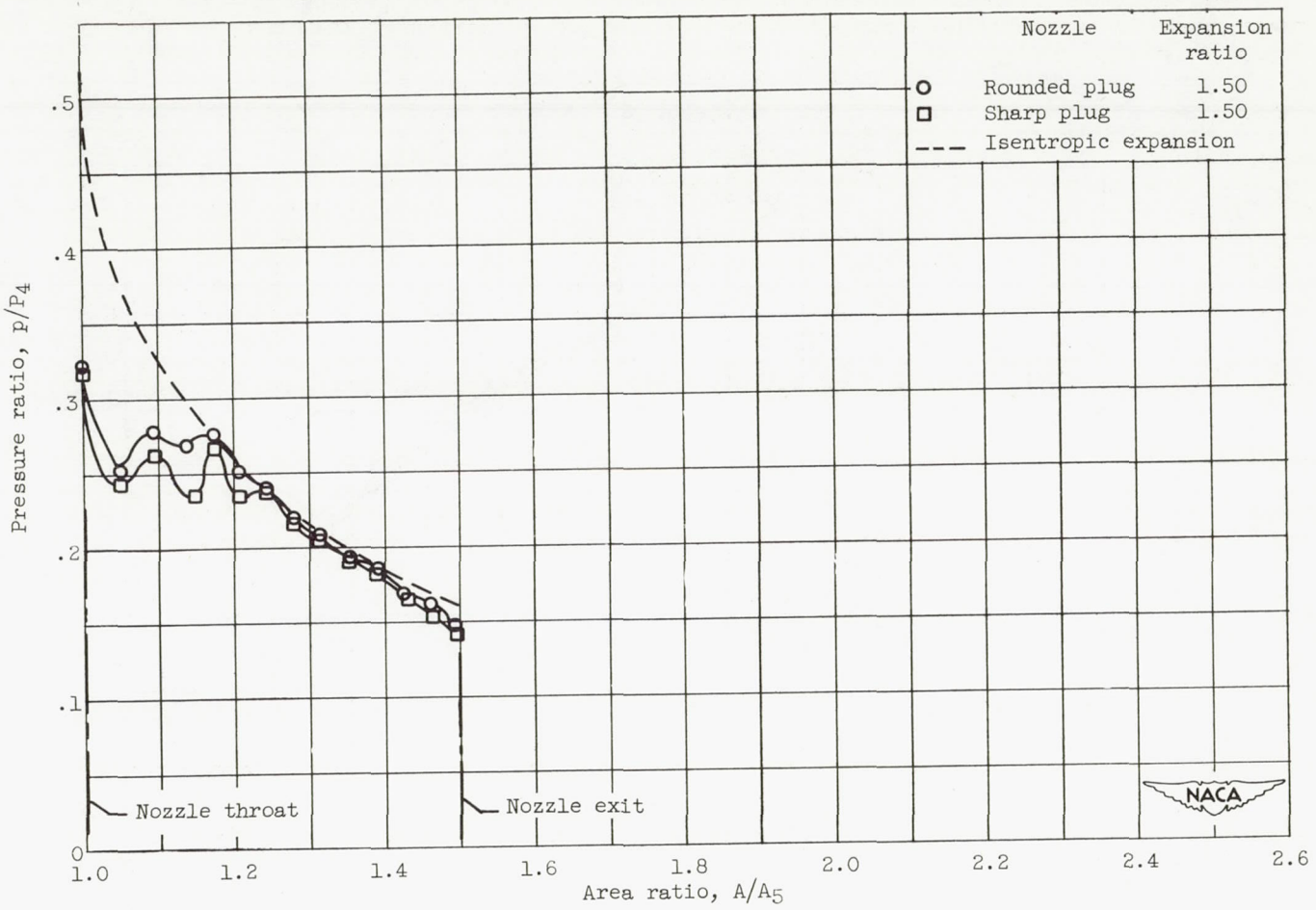
(d) Expansion ratio, 1.8.

Figure 7. - Continued. Comparison of pressure distribution along diverging walls of movable shell for completely expanded rounded-plug and sharp-plug variable-area convergent-divergent nozzles.



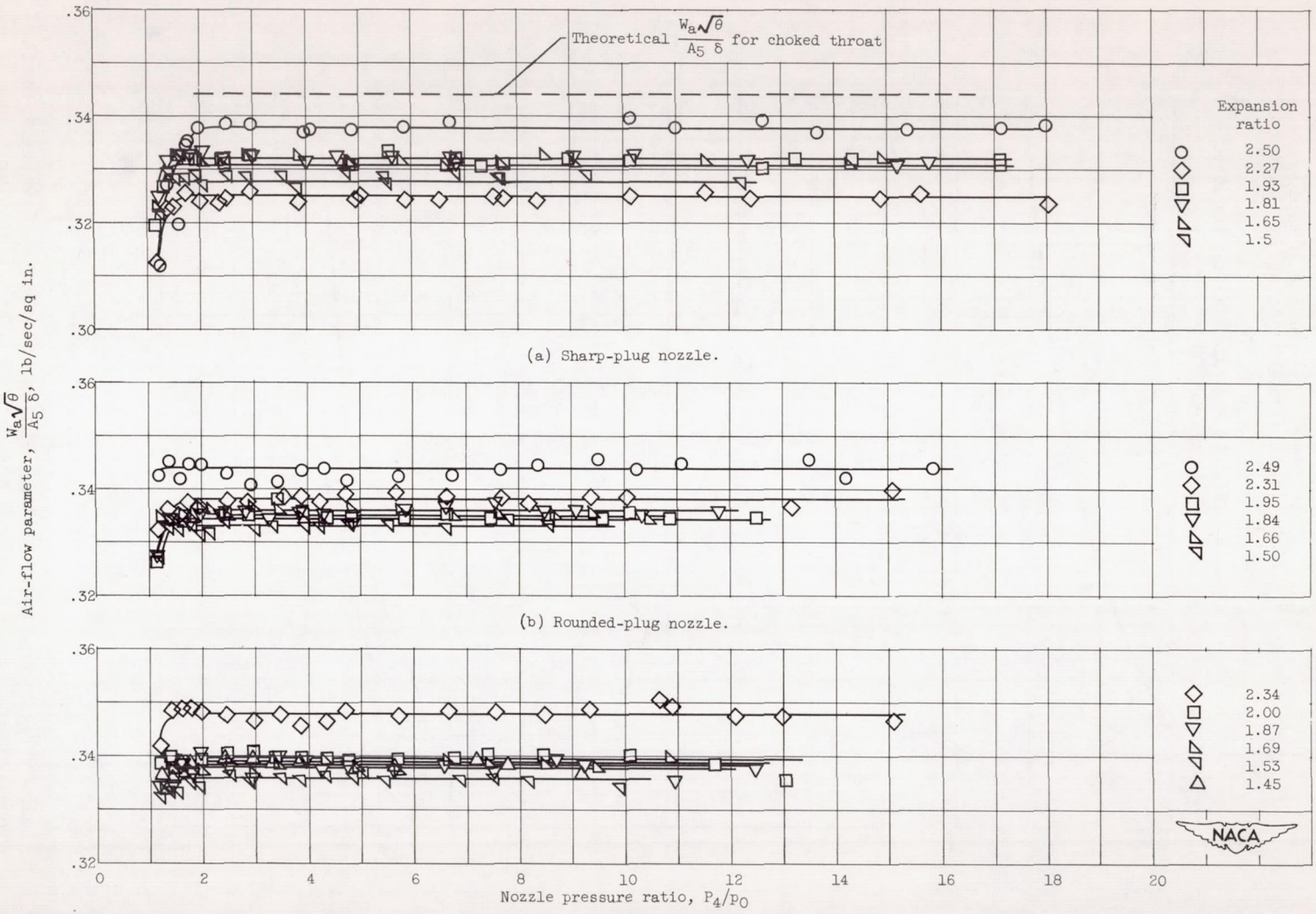
(e) Expansion ratio, 1.65.

Figure 7. - Continued. Comparison of pressure distribution along diverging walls of movable shell for completely expanded rounded-plug and sharp-plug variable-area convergent-divergent nozzles.



(f) Expansion ratio, 1.5.

Figure 7. - Concluded. Comparison of pressure distribution along diverging walls of movable shell for completely expanded rounded-plug and sharp-plug variable-area convergent-divergent nozzles.



(a) Sharp-plug nozzle.

(b) Rounded-plug nozzle.

(c) Vaned nozzle.

Figure 8. - Variation of air-flow parameter with nozzle pressure ratio for sharp-plug, rounded-plug and vaned-type variable area convergent-divergent nozzles.

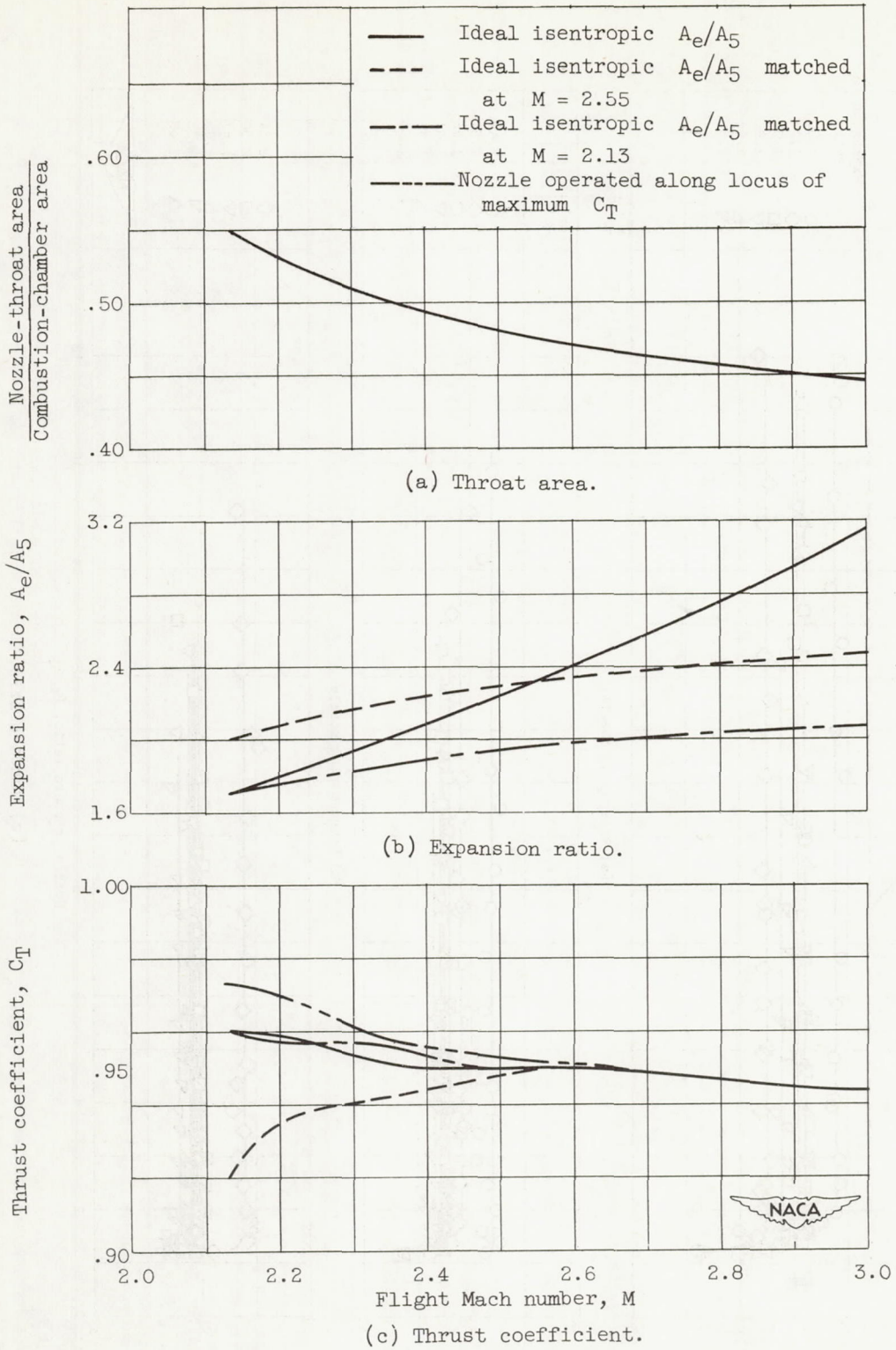


Figure 9. - Rounded-plug variable-throat convergent-divergent nozzle characteristics for typical ram-jet-missile flight plan.